Selective growth of RuO_2 nanorods and influence of thermal heating on their field emission properties

Dah-Shyang Tsai[*]*, Chih-Sung Hsieh, Ginny Wang,*
Department of Chemical Engineering, National Taiwan University of Science and Technology, Taipei, Taiwan
Reui-San Chen, Ying-Sheng Huang,
Department of Electronic Engineering, National Taiwan University of Science and Technology, Taipei, Taiwan
** corresponding author email address: tsai@ch.ntust.edu.tw*

Extended Abstract

Ruthenium dioxide which crystallizes in tetragonal rutile structure exhibits metallic conductivity at room temperature, bulk resistivity 35 μΩ-cm, which is lower than that of titanium metal. Its electrical conductivity plus the high thermal and chemical stability of oxide materials appeals to a variety of applications in electronics and catalysis.

Area selective CVD is a chemical technique to realize patterning thin films, which are essential for many electronic and miniaturized electrical devices. The room-temperature conductive RuO_2 is a legitimate candidate for fabricating durable field-emission arrays. Owing to its oxide nature, it could be an ideal material for durable field emitters. In this paper, we report the preliminary findings on selective growth of RuO_2 nanorods and their field emission properties.

RuO_2 depositions were carried out in a cold-wall reactor, using an organometallic liquid precursor Bis(ethylcyclopentadienyl) ruthenium (Strem chemical). Temperatures of the precursor reservoir and the transport tube were controlled between 150 and 180°C to avoid precursor condensation during vapor transport. High purity oxygen at flow rate 20 sccm was the carrier gas. The substrate temperature was set between 440 and 540°C and the chamber pressure was between 1 and 4 mbar for RuO_2 deposition. For area-selective growth of thin films or nanorods, the substrate temperature range was 480 - 540°C. The selective growth of nanorods, instead of thin film, the temperature range was further restricted, 500±10°C.

Blankets of RuO_2 nanorods can be vertically grown on $LiNbO_3$(100) single crystal at substrate temperature 440-520°C. The (100) plane of LNO crystal is chosen intentionally to erect these nanorods. Figure 1 illustrates a cross-sectional view of aligned nanorods grown at 500°C and its X-ray diffraction pattern. Since the nanorods grow in the [001] direction of

rutile and their growth direction is perpendicular to the single crystal substrate, the (002) reflection is the only prominent RuO_2 reflection in the diffraction pattern besides the (003) reflection of LNO substrate.

Blanket growth of RuO_2 nanorods has also been carried out on the Zn/Si substrate in the same temperature range. The oxidized zinc metal provides nucleation sites for nanorods, but does not align these nanorods. Figure 2 depicts a typical 45° view of nanorods grown on Zn/Si substrate and its XRD diffraction pattern. Present are the reflections of (110), (101), (200), (111), (211), (220), and (002), which include all the RuO_2 reflections between 2θ=25 and 65°. The intensity of (101) reflection is particularly strong, compared with the JCPDS pattern (No. 88-0322). Since the (101) reflection comes from the sidewalls of nanorods, we can infer that most of grown nanorods are tilted with respect to the Zn/Si substrate.

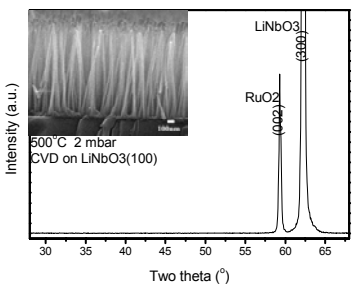

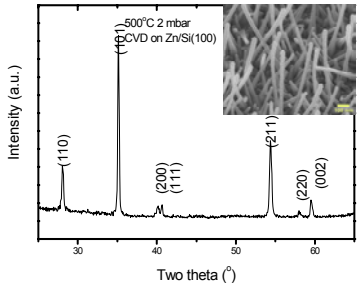

Fig.1 XRD pattern and image of RuO_2 nanorods vertically aligned on LNO(100). Fig.2 XRD pattern and image of RuO2 nanorods on Zn/Si substrate.

The area-selective growth of RuO_2 nanorods can be achieved when the LNO(100) (or Zn/Si) surface and the silica surface are present simultaneously in CVD. The selectivity originates from the energy barrier on silica surface that prohibits RuO_2 nucleation. The nanorods pattern in Fig. 2(A) is formed, since the sputtered silicon square patch on the masked area has been oxidized and the impinging Ru-containing species are difficult to nucleate on the newly formed SiO_2/LNO surface. On the other hand, the Ru-containing species quickly adsorb and deposit on the unmasked LNO(100) area. A thin RuO_2 film soon establishes and serves as the root layer for growing RuO_2 nanorods. Those grains with (001) plane facing the gas phase will grow upwards faster than other grains and turn into nanorods. An inversed pattern is created in Fig. 2(B), using the similar reasoning, except that the area being covered by copper grids is oxidized into SiO_2/Si, the nongrowth surface. And the square patches without being covered is sputtered with zinc and oxidized into the growth surface.

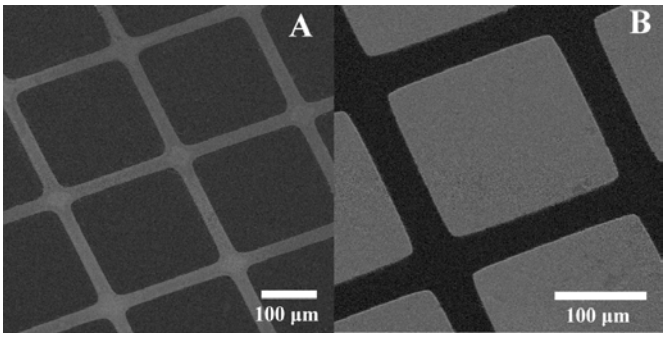

Fig.2 Patterned growth of RuO_2 nanorods using 100 mesh copper grids on (A) $LiNbO_3$ and (B) Zn/Si substrate.

The nanorods on patterned $LiNbO_3$(100) near the boundary between the growth and the nongrowth regions exhibit variations in alignment. Figure 3 illustrates the alignment variation in RuO_2 nanorods patterned by a 100 mesh copper grid. The alignment variation in nanorods gives rise to a subtle shade difference in the center of crossroad, shown in Fig. 3(A). Two rectangular zones in Fig. 3(B), zone II and III are chosen for detailed examination. Zone II is located 12 μm away from the nongrowth surface. The orientation of nanorods in zone II is the same with that of blanket-grown nanorods, which are perpendicular to the substrate, as depicted in Fig 3(C). The larger zone III is closer to the nongrowth surface, at approximately 3 μm away. Fig. 3(D) exhibits more details of zone III. The orientation of nanorods in zone III displays a continuous variation from the vertical orientation at upper left corner to the chaotic orientation at lower right corner. The number density of nanorods also appears to be decreasing in the same direction.

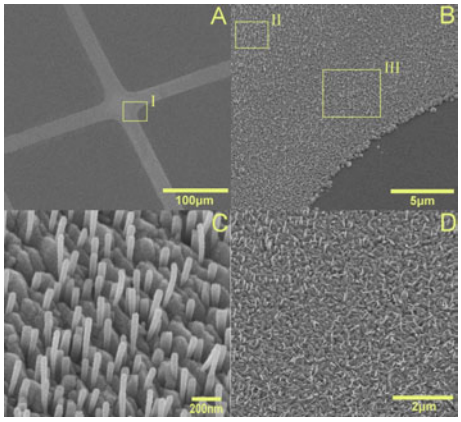

Fig. 3 Alignment of area-selectively grown RuO_2 nanorods, (A) nanorods grown at the crossroad of patterned $LiNbO_3$ using a 100 mesh copper grid, (B) nanorods grown in the rectangular area marked as I, (C) vertical grown nanorods in the rectangular area marked as II, (D) nanorods of varying orientations in the rectangular area marked as III.

The field emission properties of RuO_2 nanorods are intimately related to its average diameter and the annealing temperature. The threshold field strength E_{thr} is defined at the turning point of Fowler-Nordheim F-N plot. The turn-on field E_{to} is the field to produce a

current of 10μA/cm^2, suitable for applications in FE display. If no annealing is imposed, the slope of F-N plot is little influenced by the average diameter of RuO_2 nanorods. Yet the E_{to} value of nanorods film is a function of the average diameter. The E_{to} value of nanorods diameter 27, 38, 48 nm are 6.8, 16.6, 22.7 V/μm individually. The E_{thr} value generally decreases with emission time, 15.0V/μm(0h), 12.3V/μm(24h), 10.8V/μm(48h), for nanorods of diameter 48 nm, Fig. 4(A).

If the nanorods film is 400°C annealed for 1h, both of the slope of F-N plot and the E_{thr} value decrease significantly with the emission time. For the nanorods film of average diameter 48 nm, the slope value decreases from 314V/μm(0h) to 133V/μm(48h). The E_{thr} value decreases from 7.8V/μm(0h) to 5.6V/μm(48h), Fig. 4(B). A similar trend can be found on the slope and the E_{thr} value of the nanorods film of 35 nm diameter. Regardless the diameter difference, the E_{thr} of annealed samples after long emission time all reach values around 5.5 V/μm. The field emission features could be related to the adsorption and desorption of gases on the nanorods during emission.

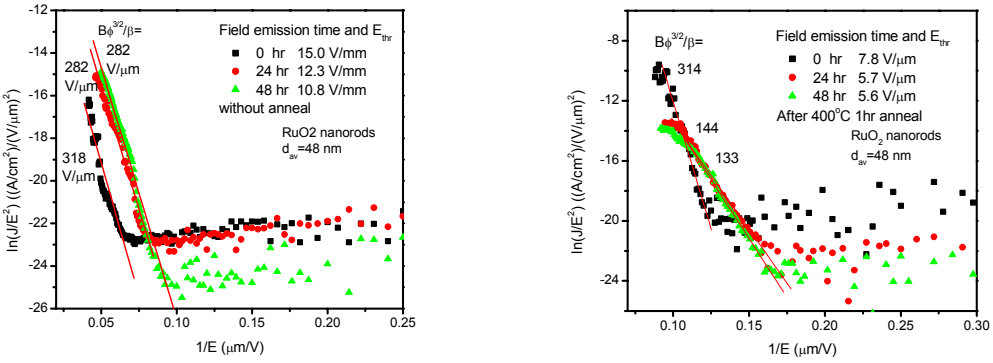

(A) (B)

Fig. 4 The F-N plot of RuO_2 nanorods film, average diameter 48 nm, (A) without thermal annealing, (B) 400°C 1h annealing.